Computer Assisted Mechanics and Engineering Sciences, 10: 339–351, 2003.

Application of Trefftz method to steady-state heat conduction problem in functionally gradient materials

Eisuke Kita
Graduate School of Information Sciences
Nagoya University

Youichi Ikeda
Department of Mechanical Engineering
Daidoh Institute of Technology

Norio Kamiya
Graduate School of Information Sciences
Nagoya University

(Received October 15, 2001)

This paper describes the application of Trefftz method to the steady-state heat conduction problem on the functionally gradient materials. Since the governing equation is expressed as the non-linear Poisson equation, it is difficult to apply the ordinary Trefftz method to this problem. For overcoming this difficulty, we will present the combination scheme of the Trefftz method with the computing point analysis method. The inhomogeneous term of the Poisson equation is approximated by the polynomial of the Cartesian coordinates to determine the particular solution related to the inhomogeneous term. The solution of the problem is approximated with the linear combination of the particular solution and the T-complete functions of the Laplace equation. The unknown parameters are determined so that the approximate solution will satisfy the boundary conditions by means of the collocation method. Finally, the scheme is applied to some numerical examples.

Keywords: Trefftz method, computing point analysis method, steady-state heat conduction, functionally gradient materials

1. Introduction

Functionally gradient material is the material of which physical property changes gradually from one surface to the other. Although the material is the composite material which combined the material of a different kind, there is no joint between different kind of materials because two materials are mixed on an atomic level. Therefore, the material is hard to break when it is stretched by the outer force. The field to which functionally gradient material is expected most is a use as super-heat resistance structure material used for a rocket engine, a space shuttle, a nuclear fusion reactor, a chemistry plant, and so on.

The steady-state heat conduction problem in the functionally gradient material can be modeled as the boundary value problem of the nonlinear Poisson equation if the heat conductivity changes gradually. When the boundary-type solution procedures such as boundary element and Trefftz methods are applied to the boundary value problem of the nonlinear Poisson equation, there exits a great difficulty due to the inhomogeneous term of the Poisson equation. In the boundary element formulation, the integral equation derived from the governing equation has the domain integral term related to the inhomogeneous term and therefore, the domain discretization is necessary.

For overcoming this difficulty, some researchers have been studying Multiple Reciprocity Method (MRM) [1, 2], Dual Reciprocity Method (DRM) [3–6], computing point analysis scheme [7, 8] and so on. In the multiple reciprocity method, the application of the Gauss–Green formula transforms the domain integral term into the infinite series of the boundary integral terms. It is proven mathematically that the solution converges to some value as the number of boundary integral terms increases. In the dual reciprocity method, the inhomogeneous term is approximated by relatively simple function. The domain integral term is transformed into the boundary integral term by using the particular solution related to the inhomogeneous term and applying the Gauss–Green formula. The inhomogeneous term of the governing equation, in the steady-state heat conduction problem in the functionally gradient material, includes the derivatives of the unknown function. In the boundary element method, the additional process to approximate the derivatives is necessary, which is somewhat difficult. For overcoming this difficulty, this paper presents the combination method of Trefftz method and the computing point analysis scheme [7–14]. Trefftz method is boundary-type solution procedure using regular T-complete functions. The solution of the problem is approximated by the linear combination of the T-complete functions and the unknown parameters are determined so that the solution satisfies the boundary condition. The authors applied the same formulation for solving the nonlinear Poisson equation in the previous studies [15, 16]. This paper describes the application of the scheme to engineering problem.

In the present method, an inhomogeneous term including the derivatives of the unknown function is approximated by the 5-order polynomial in Cartesian coordinates to derive the particular solution related to the inhomogeneous term. The use of the particular solution transforms the boundary value problem of the Poisson equation into that of the Laplace equation. Once the Laplace problem is solved for the homogeneous solution by the boundary data alone, the solution of the problem is estimated from the homogeneous and the particular solutions. Since, in Trefftz method, the unknown function is approximated with the linear combination of the regular T-complete functions, direct differentiation of the approximate expression leads to its derivatives. This process is straightforward and easier than the boundary element method. Finally, we shall consider as the numerical examples the functionally gradient materials of which heat conductivities are a linear and quadratic functions in order to examine the property.

2. Formulation

2.1. Governing equation and boundary conditions

When the heat conductivity λ is given as a continuous function, the steady-state heat conduction problem of the functionally gradient material can be modeled by the governing equation:

$$\nabla\{\lambda\nabla u\} = 0 \quad (\text{in } \Omega) \tag{1}$$

and the boundary conditions:

$$\left.\begin{aligned} u &= \overline{u} \quad (\text{on } \Gamma_u) \\ q &= \overline{q} \quad (\text{on } \Gamma_q) \end{aligned}\right\} \tag{2}$$

where $q \equiv \partial u/\partial \mathbf{n}$ and Ω, Γ_u and Γ_q denote the object domain under consideration, its potential u and the flux q specified boundaries, respectively. $\mathbf{n}$ denotes the unit normal vector on the boundary and $(\bar{\cdot})$ the specified value.

Equation (1) can be expanded as follows.

$$\nabla^2 u + \frac{1}{\lambda}\nabla\lambda\nabla u = 0, \tag{3}$$

where the second term of the left-hand side is defined as

$$b = \frac{1}{\lambda}\nabla\lambda\nabla u. \tag{4}$$

The term b means an inhomogeneous term for the inhomogeneous property of the material. In the traditional boundary element formulation, the integral equation has the domain integral term related to the inhomogeneous term.

2.2. Transformation of differential equation

The inhomogeneous term b is approximated by 5-order complete function of the Cartesian coordinates;

$$\begin{aligned} b &= c_1 + c_2 x + c_3 y + \cdots + c_{20} x y^4 + c_{21} y^5 \\ &= \mathbf{c}^T \mathbf{r}, \end{aligned} \tag{5}$$

where $\mathbf{c}$ and $\mathbf{r}$ mean the unknown parameter and the coefficient vectors, respectively, which are defined as

$$\mathbf{c}^T = \{c_1, c_2, \cdots, c_{21}\}, \tag{6}$$

$$\begin{aligned} \mathbf{r}^T &= \{r_1, r_2, \cdots, r_{21}\} \\ &= \{1, x, y, x^2, xy, y^2, x^3, x^2 y, x y^2, y^3, x^4, x^3 y, x^2 y^2, x y^3, y^4, x^5, x^4 y, x^3 y^2, x^2 y^3, x y^4, y^5\}. \end{aligned} \tag{7}$$

Applying Eq. (5) to (3), we have

$$\nabla^2 u + \mathbf{c}^T \mathbf{r} = 0. \tag{8}$$

Assuming the homogenous solution of Eq. (8) as u^h and the particular solution related to r_i as u_i^p, the solution of the problem u is given as

$$\begin{aligned} u &= u^h + c_1 u_1^p + c_2 u_2^p + \cdots + c_{21} u_{21}^p \\ &= u^h + \mathbf{c}^T \mathbf{u}^p, \end{aligned} \tag{9}$$

where $\mathbf{u}^p = \{u_1^p, u_2^p, \cdots, u_{21}^p\}^T$ and u^h and u_i^p satisfy the following equations.

$$\nabla^2 u^h = 0, \tag{10}$$

$$\nabla^2 u_i^p + r_i = 0. \tag{11}$$

Since r_i is polynomial, the particular solution u_i^p can be estimated easily.

Substituting Eq. (9) to Eqs. (3) and (2), the boundary value problem can be transformed into

$$\nabla^2 u^h = 0 \quad (\text{in } \Omega) \tag{12}$$

and

$$\left.\begin{aligned} u^h &= \overline{u} - \mathbf{c}^T \mathbf{u}^p \equiv \overline{u}^h \quad (\text{on } \Gamma_1) \\ q^h &= \overline{q} - \mathbf{c}^T \mathbf{q}^p \equiv \overline{q}^h \quad (\text{on } \Gamma_2) \end{aligned}\right\} \tag{13}$$

where $q^h \equiv \partial u_i^h / \partial \mathbf{n}$ and $q_i^p \equiv \partial u_i^p / \partial \mathbf{n}$.

2.3. Trefftz formulation of two-dimensional Laplace equation

Trefftz method is formulated by using the non-singular T-complete function. T-complete functions are determined so as to satisfy the governing equation [12];

$$\begin{aligned}\mathbf{u}^* &= \{u_1^*, \cdots, u_{2\mu-1}^*, u_{2\mu}^*, \cdots\}^T \\ &= \{1, \cdots, \Re[z^\mu], \Im[z^\mu], \cdots\}^T,\end{aligned} \tag{14}$$

where $z = x + jy$ and $j = \sqrt{-1}$.

The potential u^h is approximated by the linear combination of the T-complete functions u_j^*;

$$\begin{aligned}u^h \simeq \widetilde{u}^h &= a_1 u_1^* + a_2 u_2^* + \cdots + a_N u_N^* \\ &= \mathbf{a}^T \mathbf{u}^*,\end{aligned} \tag{15}$$

where N is the total number of the T-complete functions and $\mathbf{a} = \{a_1, \cdots, a_N\}^T$ denotes the unknown parameter vector. Direct differentiation of the above equation leads to the approximate expression of the flux:

$$\begin{aligned}q^h \simeq \widetilde{q}^h \equiv \frac{\partial \widetilde{u}^h}{\partial n} &= a_1 q_1^* + a_2 q_2^* + \cdots + a_N q_N^* \\ &= \mathbf{a}^T \mathbf{q}^*.\end{aligned} \tag{16}$$

Since the T-complete functions are determined so as to satisfy the governing equation, Equations (15) and (16) satisfy Eq. (12). They do not satisfy the boundary condition (13) and therefore, the residuals yield:

$$\left.\begin{array}{lcll} R_u & \equiv & \widetilde{u}^h - \overline{u}^h = \mathbf{a}^T \mathbf{u}^* - \overline{u}^h \neq 0 & \text{on } \Gamma_u \\ R_q & \equiv & \widetilde{q}^h - \overline{q}^h = \mathbf{a}^T \mathbf{q}^* - \overline{q}^h \neq 0 & \text{on } \Gamma_q \end{array}\right\}.$$

In this study, the unknown parameter $\mathbf{a}$ is determined so that the residuals are minimized by means of the collocation method. The residuals R_u and R_q are forced to be zero at the boundary collocation point P_i, so we have

$$\left.\begin{array}{lcl} R_u(P_i) & = & \mathbf{a}^T \mathbf{u}^*(P_i) - \overline{u}^h(P_i) = 0 \quad (P_i \in \Gamma_u) \\ R_q(P_i) & = & \mathbf{a}^T \mathbf{q}^*(P_i) - \overline{q}^h(P_i) = 0 \quad (P_i \in \Gamma_q) \end{array}\right\}.$$

By rearranging the equation, we have

$$\mathbf{K}\mathbf{a} = \mathbf{f}, \tag{17}$$

where

$$\mathbf{K} = \begin{bmatrix} u_{11}^* & \cdots & u_{1N}^* \\ \vdots & & \vdots \\ u_{M_u 1}^* & \cdots & u_{M_u N}^* \\ q_{11}^* & \cdots & q_{1N}^* \\ \vdots & & \vdots \\ q_{M_q 1}^* & \cdots & q_{M_q N}^* \end{bmatrix}, \tag{18}$$

$$\mathbf{f} = \{\overline{u}_1, \cdots, \overline{u}_{M_u}, \overline{q}_1, \cdots, \overline{q}_{M_q}\}^T, \tag{19}$$

$u_j^*(P_i) \equiv u_{ij}^*, q_j^*(P_i) \equiv q_{ij}^*, \overline{u}(P_i) \equiv \overline{u}_i, \overline{q}(P_i) \equiv \overline{q}_i$. M_u and M_q mean the total numbers of the collocation points on the boundaries Γ_u and Γ_q, respectively. The row and the column of the coefficient matrix $\mathbf{K}$ are equal to the total numbers of the collocation points and the T-complete functions, respectively. Equation (17) is solved by the singular value decomposition [17].

2.4. Update rule of unknown parameter c

The previous section describes the Trefftz formulation for the boundary value problem of two-dimensional Laplace equation. The boundary value problem defined by Eqs. (12) and (13) includes the unknown parameter $\mathbf{c}$. Since $\mathbf{c}$ depends on the unknown function u, the iterative process is necessary for solving the problem. We shall describe here the iterative process.

Holding Eq. (5) at the iteration steps (k) and $(k+1)$, we have

$$b^{(k+1)} = \mathbf{r}^T \mathbf{c}^{(k+1)},$$
$$b^{(k)} = \mathbf{r}^T \mathbf{c}^{(k)}.$$

Subtracting both sides of the equations, we have

$$b^{(k+1)} - b^{(k)} = \mathbf{r}^T (\mathbf{c}^{(k+1)} - \mathbf{c}^{(k)}) \equiv \mathbf{r}^T \Delta \mathbf{c}. \tag{20}$$

$\Delta \mathbf{c}$ is determined so that Eq. (20) is satisfied by means of the collocation method at the collocation points placed in the domain and on the boundary, which are referred as "computing point". Equation (20) is held at the computing point Q_i;

$$\mathbf{r}^T(Q_i)\Delta \mathbf{c} = b^{(k+1)} - b^{(k)} = b(u^{(k)}) - \mathbf{r}^T \mathbf{c}^{(k)} \equiv \Delta b(Q_i).$$

The above equation is held at all computing point to be assembled as

$$\mathbf{D}\Delta \mathbf{c} = \mathbf{f}, \tag{21}$$

where $\mathbf{D}$ and $\mathbf{f}$ mean the coefficient matrix and vector. Equation (21) is solved for $\Delta \mathbf{c}$ by the singular value decomposition [17].

The parameter $\mathbf{c}$ is updated by

$$\mathbf{c}^{(k+1)} = \mathbf{c}^{(k)} + \Delta \mathbf{c}. \tag{22}$$

The convergence criterion is defined as

$$\eta \equiv \frac{1}{M_c} \sum_{i=1}^{M_c} |\Delta b(Q_i)| < \eta_c, \tag{23}$$

where η_c is the positive number specified by a user.

The inhomogeneous term includes the derivative of the unknown function u^h. In the Trefftz method, the function u^h is approximated by Eq. (15) and therefore, direct differentiation of Eq. (15) leads to the expression of the derivatives:

$$u_{,k} = \mathbf{a}^T \mathbf{u}^*_{,k}, \tag{24}$$

where $k = x$ or y and $(\cdot)_{,k}$ means the partial differentiation with respect to k. Since $\mathbf{u}^*$ is a regular function, it is easy to analytically differentiate $\mathbf{u}^*$ with respect to r and θ;

$$\frac{\partial \mathbf{u}^*}{\partial x} = \{0, \cdots, \Re[\mu z^{\mu-1}], \Im[\mu z^{\mu-1}], \cdots\}, \tag{25}$$

$$\frac{\partial \mathbf{u}^*}{\partial y} = \{0, \cdots, \Re[j\mu z^{\mu-1}], \Im[j\mu z^{\mu-1}], \cdots\}. \tag{26}$$

2.5. Algorithm of present scheme

The algorithm of the present scheme is as follows:

1. Set $k \leftarrow 0$ and assume $\mathbf{c}^{(0)}$.
2. Solve the boundary value problem defined by Eqs. (12) and (13) and estimate inhomogeneous term b at the computing points.
3. Check the convergence criterion (23). If the condition is satisfied, the results are printed out. If not so, the process goes to the next.
4. Solve Eq. (21) for $\Delta\mathbf{c}$.
5. Update $\mathbf{c}$ by Eq. (22) and set $k \leftarrow k+1$.
6. Go to step 2.

3. Numerical examples

3.1. Exmaple 1

We shall consider as the first example that the heat conductivity λ is a linear function in x-coordinate;

$$\lambda = d_1 + d_2 x,$$

where d_1 is specified to be 200 and d_2 is taken as 20, ± 100, ± 140. The governing equation, in this case, is given as

$$\nabla^2 u + \frac{d_2}{d_1 + d_2 x}\frac{\partial u}{\partial x} = 0.$$

The boundary condition is specified as shown in Fig. 1.

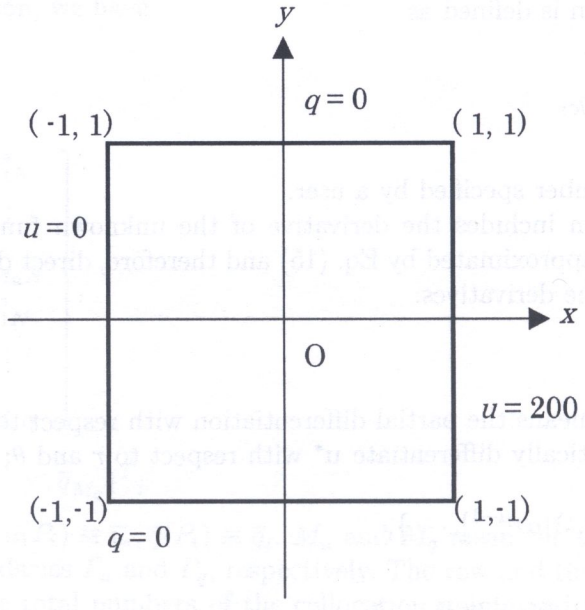

Fig. 1. Numerical example

The theoretical solution is as

$$u^{ex} = 200 \cdot \frac{\ln\left[(d_1 + d_2 x)/(d_1 - d_2)\right]}{\ln\left[(d_1 + d_2)/(d_1 - d_2)\right]}.$$

The analysis is carried out with 15 T-complete functions, 44 boundary collocation and 0, 1, 9 or 17 inner points. The placement of the points is shown in Fig. 2. All boundary collocation and inner points are taken as the computing points. The initial values of the parameter c_i is specified as zero.

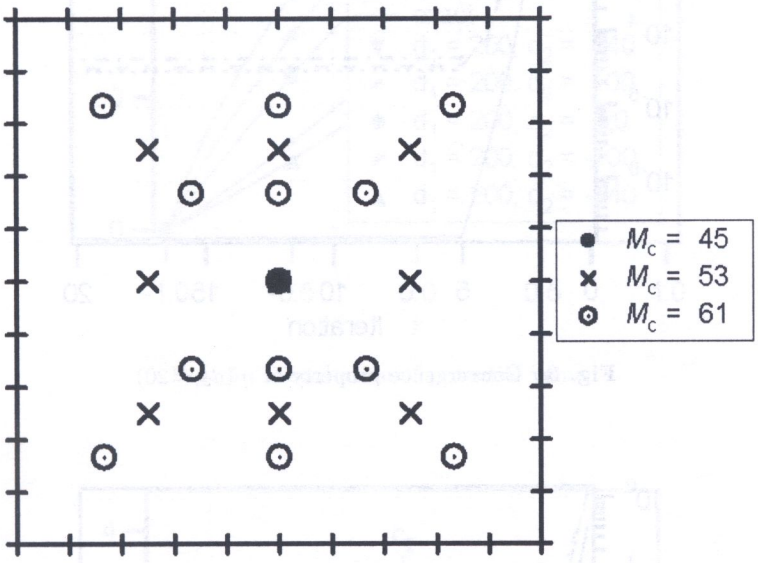

Fig. 2. Placement of collocation and computing points

The computational error is estimated at the 25 estimation points which are distributed uniformly in the object domain. One can take as the error estimator, the absolute error estimator

$$E_u^1 = \frac{1}{25} \sum |u - u^{ex}|$$

or the relative error estimator

$$E_u^1 = \frac{1}{25} \sum \left|1 - \frac{u}{u^{ex}}\right|.$$

This paper employs the absolute error estimator because u^{ex} is zero on the part of the boundary.

Figure 3 shows the convergence history of η in the case of $d_2 = 20$. The abscissa and the ordinate indicate the number of the iteration and η, respectively. In all cases, η converges at 5 iteration step. The converged value in the case of $M_c = 61$ inner points is much smaller than the other cases. Figure 4 shows the convergence history of E_u. The abscissa and the ordinate indicate the number of the iteration and E_u, respectively. The iteration step at which E_u converges to any value increases and the final value of E_u decreases as the number of the inner points increases. At the different values of d_2, the analysis is carried out by $M_c = 61$ points. Figure 5 shows the distribution of u. The abscissa and the ordinate indicate the x-coordinate of the estimation points and u, respectively. We notice that the numerical solutions well agree with the theoretical ones.

Figure 6 shows the convergence history of the parameter c_i in the case of $d_2 = 20$ and $M_c = 61$. We notice that all parameters c_i converge to any value at a few iterations. The parameters finally

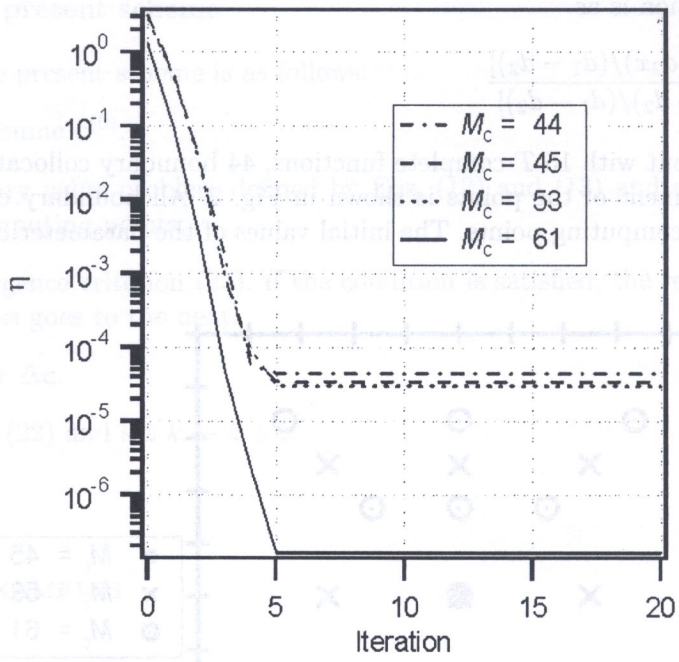

Fig. 3. Convergence property of η ($d_2 = 20$)

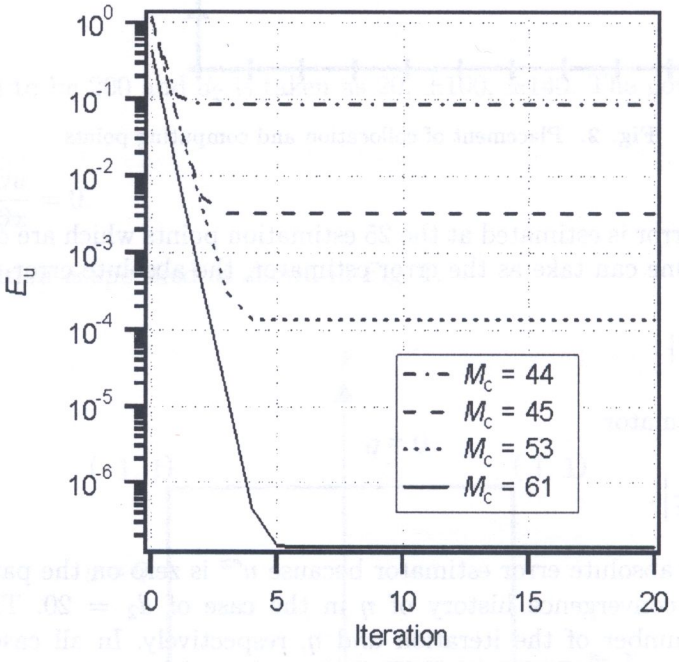

Fig. 4. Convergence property of E_u ($d_2 = 20$)

converge as follows; $c_1 \simeq -9.97$, $c_2 \simeq 1.99$, $c_4 \simeq -0.299$, $c_7 \simeq 0.0399$ and the other to almost zero. Therefore, from Eq. (5), the inhomogeneous term is predicted numerically as follows:

$$\begin{aligned} b_{\text{num}} &= c_1 + c_2 x + c_3 y + c_4 x^2 + c_5 xy + c_6 y^2 + c_7 x^3 \\ &\quad + c_8 x^2 y + c_9 xy^2 + c_{10} y^3 + c_{11} x^4 + \cdots \\ &\simeq -9.97 + 1.99x - 0.299x^2 + 0.0399x^3. \end{aligned}$$

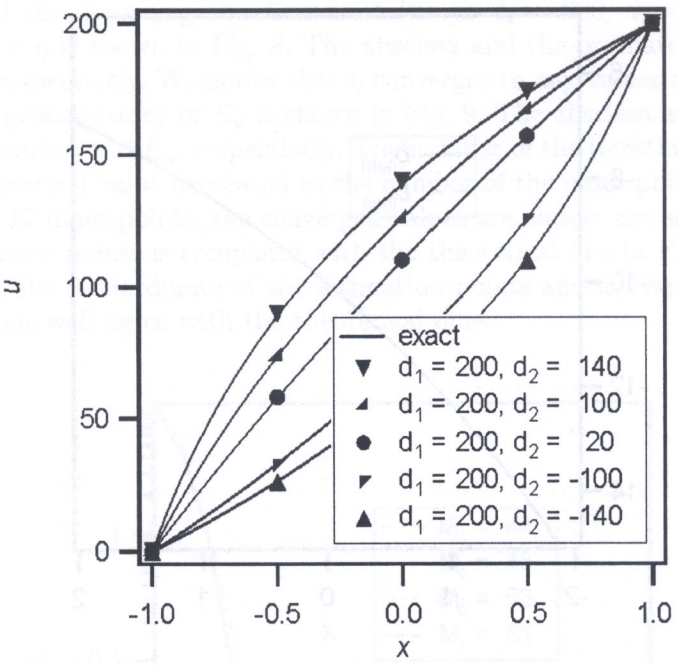

Fig. 5. Distribution of potential value

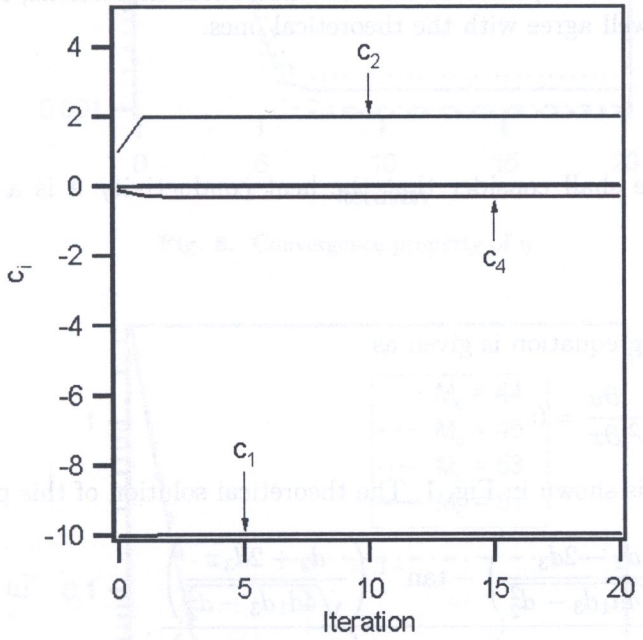

Fig. 6. Convergence property of c_i ($d_2 = 20$, $M_c = 61$)

The theoretical expression of the homogenous term is calculated from the numerical solution as follows:

$$b_{\text{theo}} = \frac{d_2}{d_1 + d_2 x} \frac{\partial u}{\partial x}$$

$$= -\frac{200}{\ln(11/9)(10+x)^2}.$$

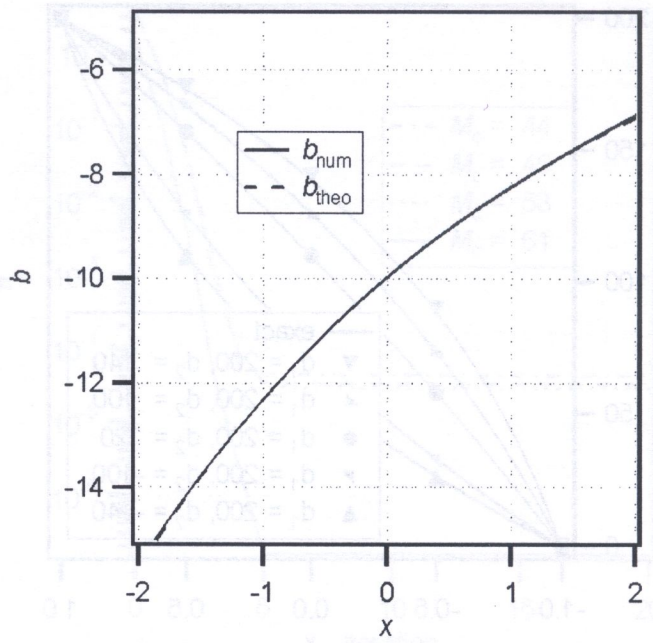

Fig. 7. Comparison of inhomogeneous term ($d_2 = 20$, $M_c = 61$)

The numerically-predicted and the theoretical expressions of the term are compared in Fig. 7. The labels b_{num} and b_{theo} denote the predicted and the theoretical expressions, respectively. We notice that the predicted term well agree with the theoretical ones.

3.2. Example 2

As the next example, we shall consider that the heat conductivity λ is a quadratic function of x-coordinate;

$$\lambda = d_1 + d_2 x + d_3 x^2.$$

In this case, the governing equation is given as

$$\nabla^2 u + \frac{d_2 + 2d_3 x}{d_1 + d_2 x + d_3 x^2} \frac{\partial u}{\partial x} = 0.$$

The boundary condition is shown in Fig. 1. The theoretical solution of this problem is given as

$$u^{ex} = 200 \cdot \frac{\tan^{-1}\left(\dfrac{d_2 - 2d_3}{\sqrt{4d_1 d_3 - d_2^2}}\right) - \tan^{-1}\left(\dfrac{d_2 + 2d_3 x}{\sqrt{4d_1 d_3 - d_2^2}}\right)}{\tan^{-1}\left(\dfrac{d_2 - 2d_3}{\sqrt{4d_1 d_3 - d_2^2}}\right) - \tan^{-1}\left(\dfrac{d_2 + 2d_3}{\sqrt{4d_1 d_3 - d_2^2}}\right)}.$$

The analysis is carried out with 15 T-complete functions, 44 boundary collocation points and 0, 1, 9 or 17 inner points. The placement of the points is shown in Fig. 2. The initial values of the parameter c_i are specified to be zero.

The computational accuracy is defined by the following error estimator estimated at 25 estimation points which are uniformly distributed in the domain under consideration.

$$E_u = \frac{1}{25} \sum |u - u^{ex}|.$$

The coefficients of the governing equation are taken as $d_1 = 200$, $d_2 = 120$ and $d_3 = 20$. The convergence history of η is shown in Fig. 8. The abscissa and the ordinate indicate the number of the iteration and η, respectively. We notice that η converges to any values at 10-th iteration step in all cases. The convergence history of E_u is shown in Fig. 9. The abscissa and the ordinate indicate the number of the iteration and E_u, respectively. The number of the iteration at which E_u converges increases and the converged value decreased as the number of the inner points increases. Especially, in the cases of 9 and 17 inner points, the converged values are almost the same. The distribution of u in the case of 17 inner points is compared with the theoretical one in Fig. 10. The abscissa and the ordinate indicate the x-coordinate of the estimation points and u, respectively. We notice that the numerical solutions well agree with the theoretical ones.

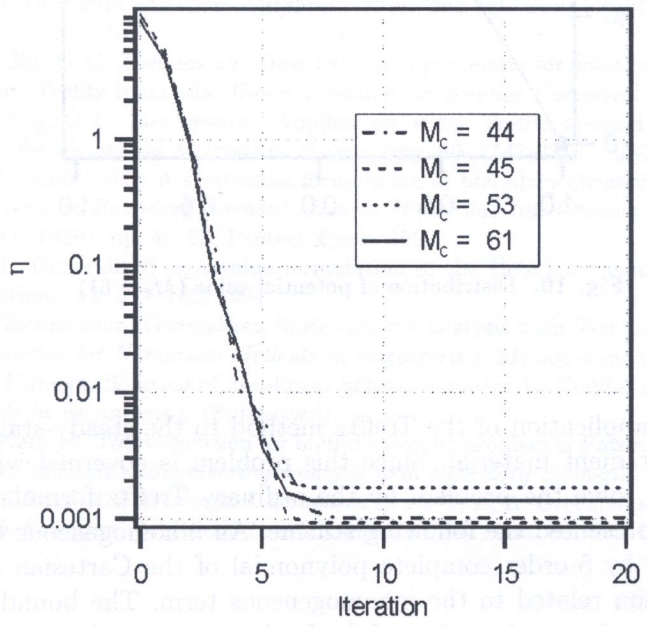

Fig. 8. Convergence property of η

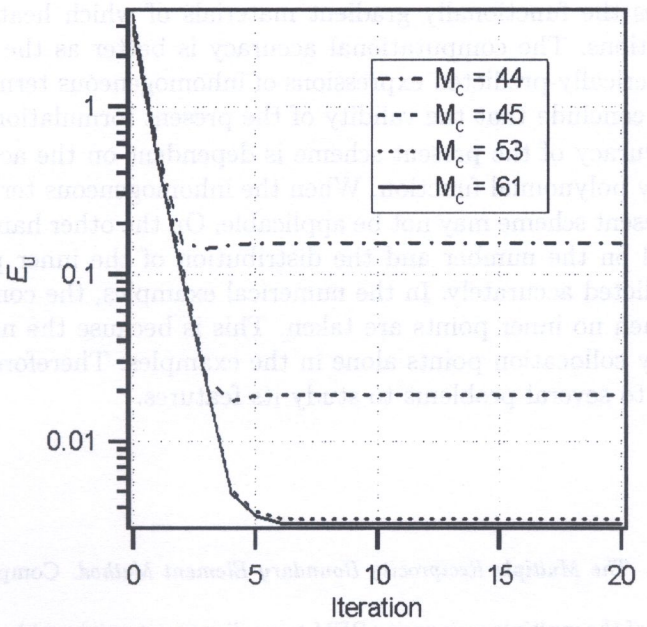

Fig. 9. Convergence property of E_u

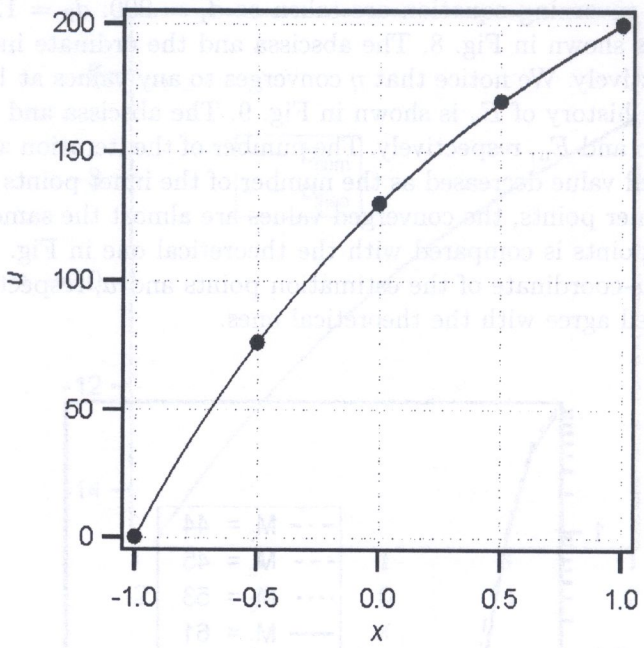

Fig. 10. Distribution of potential value ($M_c = 61$)

4. Conclusions

This paper describes the application of the Trefftz method to the steady-state heat transfer problem of the functionally gradient material. Since this problem is governed with nonlinear Poisson equation, it is difficult to solve the problem by the ordinary Trefftz formulation. For overcoming this difficulty, this paper presented the following scheme. An inhomogeneous term of the governing equation is approximated by 5-order complete polynomial of the Cartesian coordinates to determine the particular solution related to the inhomogeneous term. The boundary value problem of the Poisson equation is transformed into that of the Laplace equation by introducing the particular solution. Since the T-complete functions of the Laplace equation are known, the boundary value problem of the Laplace equation can be solved easily for the homogeneous solution. We considered as the numerical examples the functionally gradient materials of which heat conductivities are a linear and quadratic functions. The computational accuracy is better as the number of the inner points increases. The numerically-predicted expressions of inhomogeneous terms well agree with the theoretical ones. We may conclude that the validity of the present formulation can be confirmed.

The computational accuracy of the present scheme is dependent on the accuracy for predicting an inhomogeneous term by polynomial function. When the inhomogeneous term is discontinuous or strongly nonlinear, the present scheme may not be applicable. On the other hand, the computational accuracy dose not depend on the number and the distribution of the inner points if only the inhomogeneous term is predicted accurately. In the numerical examples, the computational accuracy is relatively good even when no inner points are taken. This is because the nonlinear term can be predicted by the boundary collocation points alone in the examples. Therefore, we are planning to apply the present scheme to several problems to study its features.

References

[1] A. J. Nowak, A. C. Neves. *The Multiple Reciprocity Boundary Element Method.* Comp. Mech. Pub. / Springer Verlag, 1994.

[2] A. J. Nowak. Application of the multiple reciprocity BEM to nonlinear potential problems. *Engineering Analysis with Boundary Elements*, **18**: 323–332, 1995.

[3] T. W. Partridge, C. A. Brebbia, L. C. Wrobel. *The Dual Reciprocity Boundary Element Method.* Comp. Mech. Pub. / Springer Verlag, 1992.

[4] C. S. Cheng, C. A. Brebbia, H. Power. Dual reciprocity method using compactly supported radial basis functions. *Communications of Numerical Methods in Engineering*, **15**: 225–242, 1999.

[5] W. Florez, H. Power, F. Chejne. Multi-domain dual reciprocity bem approach for the navier-stokes system of equations. *Communications in numerical methods in engineering*, **16**: 10, 671–682, 2000.

[6] K. M. Singh and M. Tanaka. Dual reciprocity boundary element analysis of inverse heat conduction problems. *Computer Methods in Applied Mechanics & Engineering*, **190**: 40, 5283–5296, 2001.

[7] S. Q. Xu, N. Kamiya. A formulation and solution for boundary element analysis of inhomogeneous-nonlinear problem. *Computational Mechanics*, **22**: 5, 367–384, 1998.

[8] S. Q. Xu, N. Kamiya. A formulation and solution for boundary element analysis of inhomogeneous-nonlinear problem; the case involving derivatives of unknown function. *Engineering Analysis with Boundary Elements*, **23**: 5/6, 391, 1999.

[9] E. Trefftz. Ein Gegenstück zum ritzschen Verfahren. *Proc. 2nd Int. Cong. Appl. Mech., Zurich*, pp. 131–137, 1926.

[10] Y. K. Cheung, W. G. Jin, O. C. Zienkiewicz. Direct solution procedure for solution of harmonic problems using complete, non-singular, Trefftz functions. *Communications in Applied Numerical Methods*, **5**: 159–169, 1989.

[11] W. G. Jin, Y. K. Cheung, O. C. Zienkiewicz. Application of the Trefftz method in plane elasticity problems. *International Journal for Numerical Methods in Engineering*, **30**: 1147–1161, 1990.

[12] I. Herrera. Theory of connectivity: A systematic formulation of boundary element methods. In: C. A. Brebbia, editor, *New Developments in Boundary Element Methods (Proc. 2nd Int. Seminar on Recent Advances in BEM, Southampton, England, 1980)*, pp. 45–58. Pentech Press, 1980.

[13] N. Kamiya, S. T. Wu. Generalized eigenvalue formulation of the Helmholtz equation by the Trefftz method. *Engineering Computations*, **11**: 177–186, 1994.

[14] A. P. Zielinski, O. C. Zienkiewicz. Generalized finite element analysis with T-complete boundary solution function. *International Journal for Numerical Methods in Engineering*, **21**: 509–528, 1985.

[15] E. Kita, Y. Ikeda, N. Kamiya. Solution of non-linear poisson equation by Trefftz method. *International Journal for Numerical Methods in Engineering.* (Submitted).

[16] E. Kita, Y. Ikeda, N. Kamiya. Trefftz solution for boundary-value problem of Poisson equation (the case involving derivatives of unknown function). *Engineering Analysis with Boundary Elements.* (Submitted).

[17] E. Anderson, Z. Bai, C. Bischof, J. Demmel, J. Dongarra, J. Du Croz, A. Greenbaum, S. Hammarling, A. McKenney, S. Ostrouchov, D. Sorensen. *LAPACK User's Manual.* SIAM, 2-nd edition, 1995.